Photoexcitation Hot Paper

International Edition: DOI: 10.1002/anie.201509252
German Edition: DOI: 10.1002/ange.201509252

Dynamics of Photoelectrons and Structural Changes of Tungsten Trioxide Observed by Femtosecond Transient XAFS

*Yohei Uemura, Daiki Kido, Yuki Wakisaka, Hiromitsu Uehara, Tadashi Ohba, Yasuhiro Niwa, Shunsuke Nozawa, Tokushi Sato, Kohei Ichiyanagi, Ryo Fukaya, Shin-ichi Adachi, Tetsuo Katayama, Tadashi Togashi, Sigeki Owada, Kanade Ogawa, Makina Yabashi, Keisuke Hatada, Satoru Takakusagi, Toshihiko Yokoyama, Bunsho Ohtani, and Kiyotaka Asakura**

Abstract: *The dynamics of the local electronic and geometric structures of WO_3 following photoexcitation were studied by femtosecond time-resolved X-ray absorption fine structure (XAFS) spectroscopy using an X-ray free electron laser (XFEL). We found that the electronic state was the first to change followed by the local structure, which was affected within 200 ps of photoexcitation.*

The utilization of solar energy is one of the most fascinating and important research subjects with regard to obtaining a society less dependent on fossil fuels. For this reason, photocatalysts and photoelectrodes[1] have been developed over the last several decades to produce hydrogen from water without the generation of harmful pollutants. More recently, tungsten trioxide (WO_3) has received much attention, since its band gap is 2.6 to 2.8 eV,[2] meaning that it functions as an active photocatalyst under visible light irradiation. WO_3 has shown the potential to allow the complete decomposition of water to hydrogen (H_2) and oxygen (O_2) when used in combination with TaON in the so-called Z-scheme photocatalyst system.[3]

Various fundamental photocatalytic properties of WO_3 have been studied by both theoretical and experimental methods. The main goal of such work has been to determine where photocarriers are created and how and when they are consumed. Density functional theory (DFT) calculations concerning the ground state[4] have shown that the valence band of WO_3 is primarily composed of O 2p orbitals and that the conduction band consists of W 5d orbitals. Electrons in the valence band are excited to the conduction band to create photocarriers (electrons and holes) by photoabsorption. These DFT results have thus provided insight into the nature of such photocarriers. The lifetimes of photocarriers in WO_3 have been studied using spectroscopic techniques with different time scales.[5] Amano et al.[5a] observed long-living photocarriers having lifetimes longer than 100 μs in WO_3 microparticles and claimed that these photocarriers such as these could contribute to the activity of the oxide for the water splitting reaction. Pesici et al.[5b] reported that more than 90% of electron–hole pairs recombined within 10 μs. Bedja et al. also observed the fast trapping of photoelectrons (within 1 ns) in colloidal WO_3.[5c]

Although previous fundamental studies have generated significant information with regard to photocarriers in WO_3, there have been no studies addressing the local electronic and geometric structure changes around W, especially in the case of photoexcited WO_3, even though such data are vital to understanding and improving the photocatalytic performance of this material. Recently,[6] we successfully observed the excited state around W in WO_3 100 ps after laser excitation, using a pump–probe X-ray absorption fine structure (XAFS) method employing a PF-AR (a single bunch operation storage ring with a time resolution of 100 ps).[6,7] Pump–probe XAFS is an element-specific, time-resolved technique capable of selectively detecting the local electronic state around X-ray absorbing atoms.[7] The energy diagram of band structure and the relation to W and O atomic orbitals are shown in Figure 1.[8] The conduction band of WO_3 is mainly composed of W 5d orbitals and the valence band of O 2p orbitals. W in WO_3 is d^0 state and the 5d orbitals are split into three t_{2g} orbitals (lower level) and two e_g orbitals (higher level) by the octahedral ligand field. Consequently, W L_{III}-edge absorption has a huge and broad peak, the so-called

[*] Prof. Y. Uemura, Dr. Y. Wakisaka, Prof. T. Yokoyama
Institute for Molecular Science
Myodaiji-cho, Okazaki 444-8585 (Japan)
D. Kido, Dr. H. Uehara, Dr. T. Ohba, Prof. S. Takakusagi, Prof. B. Ohtani, Prof. K. Asakura
Institute for Catalysis Hokkaido University
Sapporo 001-0021 (Japan)
E-mail: askr@cat.hokudai.ac.jp
Dr. Y. Wakisaka
Graduate School of Science, Nagoya University
Nagoya (Japan)
M.Sc. Y. Niwa, Dr. S. Nozawa, Dr. T. Sato, Dr. K. Ichiyanagi, Dr. R. Fukaya, Prof. S.-i. Adachi
PF, IMSS, KEK
Tsukuba 305-0801 (Japan)
Dr. T. Katayama, Dr. T. Togashi
JASRI, Kouto
Sayo-cho, Hyogo 679-5198 (Japan)
Dr. S. Owada, Dr. K. Ogawa, Dr. M. Yabashi
RIKEN SPring-8 Center, Kouto
Sayo-cho, Hyogo 679-5148 (Japan)
Dr. K. Hatada
Département Matériaux Nanosciences,Institut de Physique de Rennes, Université de Rennes1
263 Av. du Général Leclerc 35042 Rennes cedex (France)
Supporting information and ORCID(s) from the author(s) for this article are available on the WWW under http://dx.doi.org/10.1002/anie.201509252.

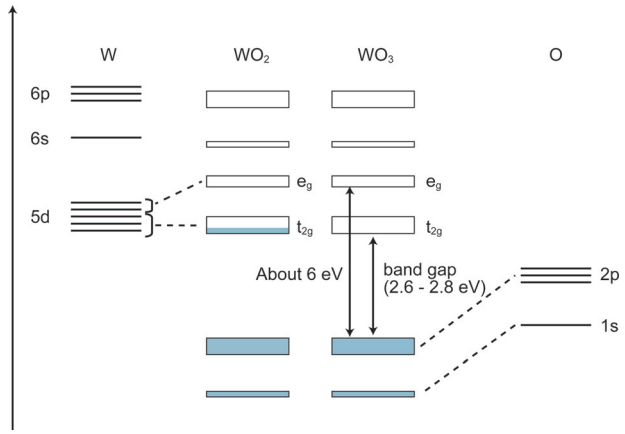

Figure 1. A schematic diagram of band structures of WO_2 and WO_3. We have added the energy difference (about 6 eV) between valence band and e_g level.[8]

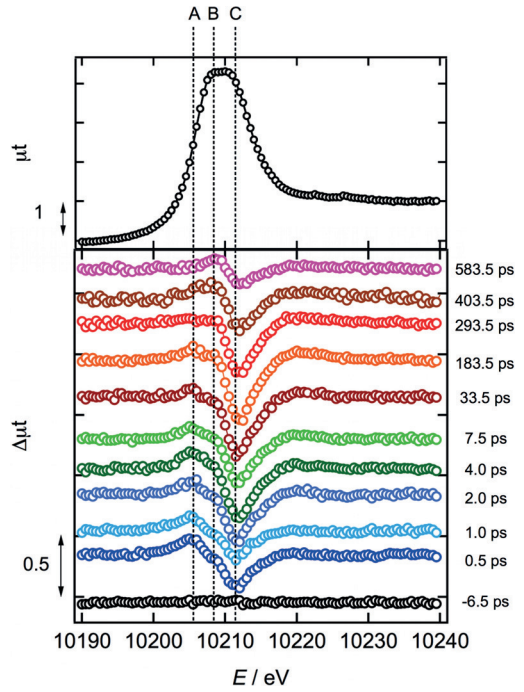

Figure 2. W L_{III} XANES spectra of WO_3 in the ground state and difference XANES spectra of WO_3. Each difference spectrum is the subtraction of the XANES spectrum of an excited state and the spectrum of a ground state. The time differences between X-ray and laser pulses are beside each spectrum. Full details in main text.

white line, as shown in Figure 2, which reflects the electronic transition from W $2p_{3/2}$ to the empty W 5d orbitals. In the previous experiments,[6] following a 400 nm laser pulse excitation, the W L_{III}-edge XAFS white line peak especially in the higher energy side dramatically decreases, directly indicating that the excited electrons occupy W e_g orbitals. However, this interpretation has a crucial problem in that the photon energy of the excitation laser (3 eV) is much lower than energy difference (>6 eV) between the valence band and the conduction band associated with the e_g state. Therefore direct photoexcitation to the e_g state should be impossible in one-photon absorption process. As such, the phenomenon we observed was instead a secondary process, indicating that a faster pump–probe XAFS experiment with a time resolution less than 100 ps was necessary. Herein, we performed femtosecond (fs) pump-probe XAFS experiments with an X-ray free electron laser (XFEL) using the SPring-8 Angstrom Compact Free Electron Laser (SACLA), which provides X-ray pulses of less than 10 fs.[9] On the basis of this work, we have found new features in the photoabsorption process and herein we present new interpretations.

The experiments were carried out at the EH2 unit of BL3 at SACLA (Proposal No. 2014B8044; 2015A8039). Si(111) double crystals were used to monochromatize the X-ray pulses and a chirped-pulse amplified laser was employed to excite the WO_3 sample. The pulse duration and wavelength of the excitation laser were 70 fs and 400 nm, respectively, while the fluence was approximately 520 mJ cm^{-2}. All the XAFS spectra were acquired in the fluorescence mode. A Kapton film was used to scatter the X-ray pulses so as to allow measurement of the incident X-ray intensity by the two photodiodes. Fluorescence X-rays emitted from the sample were also measured by a photodiode. A beryllium thin film was placed in front of the photodiode to avoid detection of scattered light from the excitation laser. The sample was a suspension of WO_3 nanoparticles in which the concentration of WO_3 was 4 mM. A continuous flow of the suspension was provided by a magnetic gear pump to prevent the sample from precipitating. The overall time resolution of the pump–probe XAFS at SACLA was 500 fs owing to a time jitter.

Figure 2 (upper) shows the W L_{III} XANES spectrum in the ground state, and Figure 2 (lower) the difference spectra between the XANES spectra of WO_3 in the ground and the excited states. Compared to previous pump–probe experiments, the signal to noise (S/N) ratios were greatly improved when using the strong XFEL pulse. Three distinct peaks are evident in the difference spectrum in Figure 2, denoted as A, B, and C. In our previous work using synchrotron radiation, we were able to identify only peak C, at 10211 eV.

Peak A at approximately 10206 eV appeared 0.5 ps (500 fs) after the excitation and was positioned just at the edge. Peak A maintained an almost constant intensity for 200 ps and then gradually decreased, as shown in Figure 3 A. Peak B appeared at 10208 eV, and the transient behavior of this peak below 200 ps was quite complicated due to the effects of the two larger peaks A and C, as can be seen in Figure 3 B. The negative peak C at 10211 eV grew rapidly and then increased more gradually up to 200 ps, followed by a decrease in its absolute intensity. The time evolution of peak C could be fitted with the sequential first-order equation $\alpha^*\exp(-k_1 t)+\beta^*\exp(-k_2 t)+\gamma$, as shown in the Figure 3 C. From the data, we estimated k_1 and k_2 to be 0.007(1) and 0.00056(5) ps^{-1}, respectively (time constant $\tau_1(=1/k_1)=140\pm 20$ ps, $\tau_2(=1/k_2)=1800\pm 200$ ps). This k_2 value is consistent with the rate constant estimated in our previous experimental work.[6] The decays of peaks A and B after 200 ps could be fitted with a single exponential, giving the same k value of 0.00056 ps^{-1}, as shown in Figure 3. All three peaks may therefore represent the same decay process. In our previous

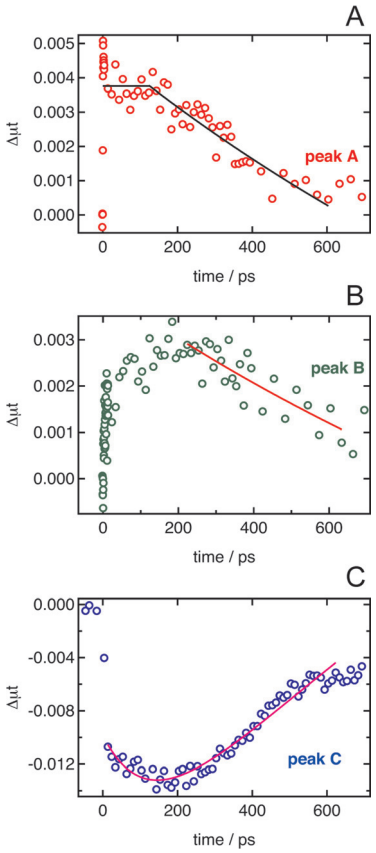

Figure 3. Changes in the absorption intensities of W L_{III} XANES peaks A, B, and C (as shown in Figure 2) with time. For the fit (colored lines) of the changes in each peak, see text.

paper, we assigned peak C to the e_g state.[6] Figure S1 presents XANES spectra for the standard compounds WO_3 and WO_2. The white line peak is seen to shift to higher energy values and to increase in intensity in conjunction with the higher oxidation state. Figure S2 shows the first and second derivatives of the raw data obtained from WO_3. The first derivative generates one positive peak and one negative peak that exhibit peak shapes and separation similar to those of the difference spectrum obtained at 0.5 ps. The pump laser evidently induced an electron transfer from O to W, resulting in the reduction of W^{VI} to W^{V} and prompting the edge shift to the lower energy side. The simple edge shift gives the positive peak at the lower energy side and negative peak at the higher energy side in the difference spectra. Assuming that no d state receives an electron, the peak shape may be approximated by the first derivative as in the equation $\Delta\mu t = d\mu t/dE \times \Delta E$. ΔE was estimated to be 0.4 eV based on the shift of the negative first-derivative peak derived from peak C. Figure S3 presents a plot of the equation $d\mu t/dE \times \Delta E$ (= 0.4 eV) in which peak C and the negative peak of the first derivative appear in the vicinity of 10212 eV and are close to one another. Peak A was much smaller than the positive peak obtained from the first derivative because of the filling of d vacancies by the excited electrons generated via the laser. We thus conclude that peaks A and C result from the energy shift of the white line. Our previous interpretation of peak C, that the photoexcited electron occupies the e_g state in the higher energy d state, should therefore be corrected.[6] Our new interpretation of the peak changes agrees with the general understanding that photoabsorption excites the valence electron primarily associated with the O 2p orbital to the bottom of the conduction band composed of the W 5d orbitals. The XAFS spectra in the excited state are shifted to lower energies due to emergence of W^{5+}. As a result, peaks A and C appear in the difference spectra. The W^{5+} state appears to be present for several picoseconds after excitation, judging from the total 5d line peak intensity change shown in Figure S5. However, the absolute value of the peak C intensity further increased over time, while peak A maintained a constant intensity up to 200 ps. At the same time, peak B also increased. These gradual changes may arise from the local structural transformations that occur along with variations in the electronic structure. The theoretically calculated XANES spectra of the ground-state WO_3 having monoclinic (room temperature form) and orthorhombic (high temperature form) structures were generated using full-potential multiple scattering (FPMS).[10] The higher energy region of the white line of the orthorhombic form is weaker in the vicinity of peak C compared to that of the monoclinic (ground state) form, as shown in Figure S4. We therefore suggest that the local structure transformation to an orthorhombic-like structure up to 200 ps. After 200 ps, the orthorhombic-like local structure gradually returns to the original monoclinic structure.

A proposed summary of the overall changes is shown in Figure 4. The first process occurs immediately after photoexcitation; once WO_3 is irradiated by the excitation laser, the electrons in the valence band (primarily the O 2p orbital) are

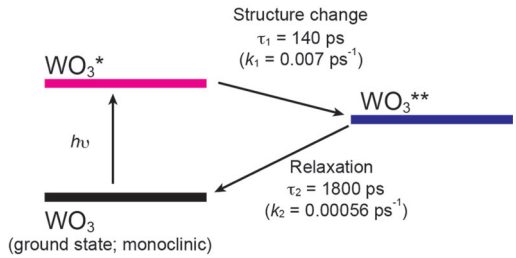

Figure 4. A proposed scheme for the photoexcitation process of WO_3.

excited to the conduction band composed of W 5d orbitals. This state is denoted as WO_3*. On average, the W was reduced to the 5.3 ± 0.3 state judging from the edge shifts or white-line area changes in Figures S5–7. The WO_3* subsequently changes its structure to that of the second excited state (WO_3**), which has less density of state (DoS) at the energy levels around peak C. Since the W–O vibrational frequency is approximately 10–20 ps^{-1} based on IR data (that is, ranges over 600–1200 cm^{-1}), this structural transformation can take place within 200 ps.

This work has shown that fs pump-probe XAFS using XFEL provides a new means of understanding the local electronic and geometric structures around a central transition element. We are now conducting pump-probe EXAFS

studies applying a wider energy range to confirm the structure change.

Acknowledgements

This work was financially supported by the JSPS through a Grant-in-Aid for Exploratory Research (No. 26620110) and by a Grant-in-Aid for Scientific Research (A) (No. 15H02173) and polymer membrane fuel cell project from NEDO. K.H. acknowledges a grant of the Marie Curie Intra-European Fellowship MS-BEEM (Grant Agreement No. PIEF-GA-2013-625388) and partial funding of FP7 MSNano network (Grant Agreement No. PIRSES-GA-2012-317554), and COST Action MP1306 EUSpec. We would like to express our thanks to Mr. Yuki Yoshimoto and Prof. Peter Krüger of Chiba University for fruitful discussions and technical support with regard to XANES calculations, and to Dr. Hiroyuki Asakura of Nagoya University for providing some of the W L_{III} XANES data.

Keywords: photoexcitation · tungsten trioxide · ultrafast spectroscopy · XAFS · X-ray free electron laser (XFEL)

How to cite: *Angew. Chem. Int. Ed.* **2016**, *55*, 1364–1367
Angew. Chem. **2016**, *128*, 1386–1389

[1] a) T. Hisatomi, J. Kubota, K. Domen, *Chem. Soc. Rev.* **2014**, *43*, 7520–7535; b) F. E. Osterloh, *Chem. Soc. Rev.* **2013**, *42*, 2294–2320; c) B. Ohtani, *Catalysts* **2013**, *3*, 942–953; d) Y. Tachibana, L. Vayssieres, J. R. Durrant, *Nat. Photonics* **2012**, *6*, 511–518; e) P. V. Kamat, *J. Phys. Chem. Lett.* **2012**, *3*, 663–672; f) K. Maeda, *J. Photochem. Photobiol. C* **2011**, *12*, 237–268; g) K. Maeda, K. Domen, *J. Phys. Chem. Lett.* **2010**, *1*, 2655–2661; h) R. Abe, *J. Photochem. Photobiol. C* **2010**, *11*, 179–209; i) A. Kudo, Y. Miseki, *Chem. Soc. Rev.* **2009**, *38*, 253–278.

[2] a) C. G. Granqvist, *Sol. Energy Mater. Sol. Cells* **2000**, *60*, 201–262; b) G. R. Bamwenda, K. Sayama, H. Arakawa, *J. Photochem. Photobiol. A* **1999**, *122*, 175–183.

[3] a) R. Abe, H. Takami, N. Murakami, B. Ohtani, *J. Am. Chem. Soc.* **2008**, *130*, 7780–7781; b) R. Abe, T. Takata, H. Sugihara, K. Domen, *Chem. Commun.* **2005**, 3829–3831.

[4] a) Y. Ping, D. Rocca, G. Galli, *Phys. Rev. B* **2013**, *87*, 165203; b) F. Wang, C. Di Valentin, G. Pacchioni, *ChemCatChem* **2012**, *4*, 476–478; c) F. Wang, C. Di Valentin, G. Pacchioni, *J. Phys. Chem. C* **2012**, *116*, 8901–8909; d) G. A. de Wijs, P. K. de Boer, R. A. de Groot, G. Kresse, *Phys. Rev. B* **1999**, *59*, 2684–2693.

[5] a) F. Amano, E. Ishinaga, A. Yamakata, *J. Phys. Chem. C* **2013**, *117*, 22584–22590; b) F. M. Pesci, A. J. Cowan, B. D. Alexander, J. R. Durrant, D. R. Klug, *J. Phys. Chem. Lett.* **2011**, *2*, 1900–1903; c) I. Bedja, S. Hotchandani, P. V. Kamat, *J. Phys. Chem.* **1993**, *97*, 11064–11070.

[6] Y. Uemura, H. Uehara, Y. Niwa, S. Nozawa, T. Sato, S. Adachi, B. Ohtani, S. Takakusagi, K. Asakura, *Chem. Lett.* **2014**, *43*, 977–979.

[7] a) M. H. Rittmann-Frank, C. J. Milne, J. Rittmann, M. Reinhard, T. J. Penfold, M. Chergui, *Angew. Chem. Int. Ed.* **2014**, *53*, 5858–5862; *Angew. Chem.* **2014**, *126*, 5968–5972; b) H. T. Lemke, C. Bressler, L. X. Chen, D. M. Fritz, K. J. Gaffney, A. Galler, W. Gawelda, K. Haldrup, R. W. Hartsock, H. Ihee, J. Kim, K. H. Kim, J. H. Lee, M. M. Nielsen, A. B. Stickrath, W. Zhang, D. Zhu, M. Cammarata, *J. Phys. Chem. A* **2013**, *117*, 735–740; c) T. Sato, S. Nozawa, A. Tomita, M. Hoshino, S.-y. Koshihara, H. Fujii, S. Adachi, *J. Phys. Chem. C* **2012**, *116*, 14232–14236; d) J. E. Katz, X. Zhang, K. Attenkofer, K. W. Chapman, C. Frandsen, P. Zarzycki, K. M. Rosso, R. W. Falcone, G. A. Waychunas, B. Gilbert, *Science* **2012**, *337*, 1200–1203; e) X. Zhang, G. Smolentsev, J. Guo, K. Attenkofer, C. Kurtz, G. Jennings, J. V. Lockard, A. B. Stickrath, L. X. Chen, *J. Phys. Chem. Lett.* **2011**, *2*, 626–632; f) J. E. Katz, B. Gilbert, X. Zhang, K. Attenkofer, R. W. Falcone, G. A. Waychunas, *J. Phys. Chem. Lett.* **2010**, *1*, 1372–1376; g) R. M. van der Veen, C. J. Milne, A. El Nahhas, F. A. Lima, V.-T. Pham, J. Best, J. A. Weinstein, C. N. Borca, R. Abela, C. Bressler, M. Chergui, *Angew. Chem. Int. Ed.* **2009**, *48*, 2711–2714; *Angew. Chem.* **2009**, *121*, 2749–2752; h) T. Sato, S. Nozawa, K. Ichiyanagi, A. Tomita, M. Chollet, H. Ichikawa, H. Fujii, S. Adachi, S. Koshihara, *J. Synchrotron Radiat.* **2009**, *16*, 110–115; i) S. Nozawa, T. Sato, M. Chollet, K. Ichiyanagi, A. Tomita, H. Fujii, S. Adachi, S. Koshihara, *J. Am. Chem. Soc.* **2010**, *132*, 61–63; j) C. Bressler, C. Milne, V. T. Pham, A. Elnahhas, R. M. Van Der Veen, W. Gawelda, S. Johnson, P. Beaud, D. Grolimund, M. Kaiser, C. N. Borca, G. Ingold, R. Abela, M. Chergui, *Science* **2009**, *323*, 489–492; k) L. X. Chen, G. B. Shaw, I. Novozhilova, T. Liu, G. Jennings, K. Attenkofer, G. J. Meyer, P. Coppens, *J. Am. Chem. Soc.* **2003**, *125*, 7022–7034; l) L. X. Chen, W. J. H. Jäger, G. Jennings, D. J. Gosztola, A. Munkholm, J. P. Hessler, *Science* **2001**, *292*, 262–264.

[8] G. A. Niklasson, C. G. Granqvist, *J. Mater. Chem.* **2007**, *17*, 127–156.

[9] a) M. Yabashi, H. Tanaka, T. Tanaka, H. Tomizawa, T. Togashi, M. Nagasono, T. Ishikawa, J. R. Harries, Y. Hikosaka, A. Hishikawa, K. Nagaya, N. Saito, E. Shigemasa, K. Yamanouchi, K. Ueda, *J. Phys. B* **2013**, *46*, 164001; b) T. Ishikawa, *Synchrotron Radiat. News* **2013**, *26*, 4–8.

[10] a) K. Hatada, K. Hayakawa, M. Benfatto, C. R. Natoli, *J. Phys. Condens. Matter* **2010**, *22*, 185501; b) K. Hatada, K. Hayakawa, M. Benfatto, C. R. Natoli, *J. Phys. Condens. Matter* **2009**, *21*, 104206.

Received: October 3, 2015
Published online: December 10, 2015

